The British Journal of Radiology, 71 (1998), 465–483

Review article

The clinical radiobiology of brachytherapy

[1]R G DALE, PhD, FIPEM and [2]B JONES, FRCP, FRCR

[1]*Hammersmith Hospitals NHS Trust, Charing Cross Hospital, London W6 8RF, and* [2]*Clatterbridge Centre for Oncology, Wirral, Merseyside L63 4JY, UK*

Abstract. The unique geometrical features of brachytherapy, together with the wide variety of temporal patterns of dose delivery, result in important interactions between physics and radiobiology. These interactions exert a major influence on the way in which brachytherapy treatments should be evaluated, both in absolute and comparative terms. This article reviews the main physical and radiobiological aspects of brachytherapy and considers examples of their influence on specific types of treatment. The issues relating to the optimization of high dose rate brachytherapy are presented, together with the implications of multiphasic repair kinetics for low dose-rate and pulsed high dose rate brachytherapy. The opportunities for application of radiobiological principles to improve various brachytherapy techniques, together with the integration of brachytherapy with teletherapy, are also outlined. Equations for the numerical evaluation of brachytherapy treatments are presented in the Appendices.

The inevitable dose gradients in brachytherapy ensure non-uniform dosage both within and outside target volumes. This could be considered as a potential disadvantage, particularly since modern teletherapy units can deliver high homogenous doses to small target volumes [1]. The continuing interest in brachytherapy stems from enhanced technological capabilities to place radiation sources accurately within and/or adjacent to tumours, usually enabling a high tumour to normal tissue dose ratio and a reduction in the volume of normal tissue irradiated.

There are numerous reports regarding the *in vitro* study of the dose rate effect [2–4] but until recently, relatively few reports of direct investigations of brachytherapy effects in patients or animal systems [5–14]. Accordingly, the biological basis of clinical brachytherapy is less well developed than is the case for teletherapy: clinical practice has evolved empirically from the pioneering days of continuous low dose rate (CLDR) radium therapy.

The introduction of fractionated high dose-rate (FHDR) brachytherapy [15–18] has prompted radiobiological debate, because of the implication that large fraction sizes would be used and because overall treatment times would be longer than the few days normally associated with CLDR [19–23]. Two of the radiobiological advantages of CLDR (reduced normal tissue damage due to use of a low dose rate, and short overall treatment time) may not be emulated in FHDR. Successful use of this modality thus requires a balancing of the potentially unfavourable radiobiological factors (*i.e.* high dose rate and extended treatment time) against favourable changes in the physical characteristics.

Brachytherapy was probably the first form of conformal therapy [24]. Nowadays, improved control of source placement and dwell times can enhance the degree of conformity [25], and interesting analytical methods (*e.g.* "natural" dose-volume histograms) have been developed for quantifying the homogeneity of a brachytherapy application [26–28]. Modern afterloading equipment allows accurate control of source position and dwell times in continuous low dose rate, high dose rate (HDR) and pulsed brachytherapy (PB). These new features require an understanding of the physical and radiobiological interactions because *optimization* of five sequential processes is ideally required in order to achieve the best therapeutic results:

(i) Accurate placement of catheter(s).
(ii) Arrangement of source dwell positions relative to target volume.
(iii) Selection of source dwell times to provide conformity.
(iv) Selection of dose delivery characteristics (*i.e.* dose rate, dose per fraction or pulse size/pulse interval) for optimal tumour and normal tissue biological doses.
(v) Scheduling of brachytherapy relative to teletherapy and other treatment modalities such as surgery or chemotherapy.

There are clinical situations where the physical dose aspects dominate the radiobiological

Received 4 December 1996 and in final form 11 November 1997, accepted 8 December 1997.

considerations, a corollary of this being that changing the radiobiological aspects of the prescription is unlikely to improve a brachytherapy application with poor treatment geometry. Similarly, simultaneous changes to the physical and radiobiological aspects (*e.g.* total dose, dose rate and applicator design) can make difficult the subsequent identification of the relative contributions of each change to the final clinical outcome [29].

For these reasons, radiobiological modelling can guide the clinical development of brachytherapy. Earlier power law equations [20, 22, 23, 30], have been superseded by the linear quadratic (LQ) model, which will be used throughout this article. This is the best available model for the quantitative assessment of clinical problems [31–33], primarily because it allows distinction to be made between the fractionation and dose rate sensitivities of different tissue types [33–37].

Modelling studies have attempted to equate the biological effects of the various brachytherapy techniques, to quantify the potential gains in tumour control produced by source dwell time optimization within a line source, and to assess methods which reduce over and under dosage of the critical target structures [21, 23, 25, 29, 32, 38–40].

One of the potential problems with the LQ model is that it may underestimate biological response at low doses per fraction (<2 Gy) [41, 42]. For normal tissues, the corresponding (theoretically derived) dose rate for such enhanced radiosensitization would be <0.5 Gy h^{-1} [43]. For all types of brachytherapy this would imply that tissues receiving dose per fraction or dose rates in the critical range might be at greater risk than suggested by LQ modelling, but the steep dose gradients will ensure that the total doses involved will be relatively small, so that the effect may not be of clinical significance. Recent work on human fibroblasts suggests a decrease in sensitivity with decreasing dose rate [44].

Radiobiological factors relevant to brachytherapy

Fractionation factors (α/β ratios)

These indicate the sensitivity of a given tumour or organ to changes in dose per fraction or dose rate. The parameters α and β (the linear and quadratic sensitivity coefficients in the LQ equation) respectively determine the initial slope and degree of downward curvature of the underlying cell survival curve [45–47]. If the dose per fraction (or dose rate) is decreased, those tissues possessing lower values of α/β will be preferentially spared relative to those with higher α/β values. Since most late-reacting normal tissues are generally believed to have lower α/β values than tumours, it follows that modulation of the fractionation or dose rate provides a powerful means for changing the therapeutic ratio. These parameters are therefore important in radiobiological intercomparisons between FHDR, CLDR and PB.

Repair rates (μ values)

Sub-lethally damaged cells have the propensity to repair if allowed sufficient time [20, 21, 48]. If further adjacent DNA damage accrues before the earlier damage has had sufficient time to repair, then the sub-lethal damage becomes lethal [32, 34]. This is a simplistic explanation of the repair process, but sufficient for understanding many aspects of clinical radiotherapy. A more mechanistic explanation of repair is provided by Curtis [49].

Detailed analyses of repair data suggest that, for critical normal tissues in particular, recovery may be multiphasic, *i.e.* with two or more exponential components [50–53], although for simplicity in modelling mono-exponential kinetics are often assumed. Average repair half-lives for mammalian tissues are usually 0.5–3 h, with increasing evidence that tumour recovery half-lives are probably shorter than those for late-reacting normal tissues [45]. In normal tissues exhibiting bi-phasic repair the faster component typically has a half-time of approximately 10–15 min [54].

The mono-exponential recovery constant (μ) is related to the repair half-life ($T_{1/2}$) by:

$$\mu = \frac{0.693}{T_{1/2}}$$

Repair rates and α/β ratios are the main parameters which influence tissue responses when the dose rate is changed [32, 43, 55]. Low dose rates imply a low ionization density in the critical targets, thus providing more opportunity for sub-lethally damaged cells to recover during the period of irradiation. At higher dose rates the greater ionization density results in more conversion of sub-lethal to lethal damage.

Radiosensitivity and SF_2

Although radiosensitivity is specified in terms of the α and β parameters in the LQ model, for CLDR and hyperfractionated HDR brachytherapy, α is the main determinant. There are several laboratory techniques for the estimation of radiosensitivity [56, 57] but SF_2 (the surviving fraction of cells after a 2 Gy exposure) is the most widely tested. The finding that SF_2 is more predictive of survival than tumour stage in stage I–III carcinoma of the cervix, treated using CLDR brachytherapy at around 1.5 Gy h^{-1} at Point A [57], probably reflects the importance of total dose in the control

of squamous tumours which have high α/β ratios [58]. The dose rate effect (β dependent) will then be much reduced. This assay cannot be expected to be so predictive for higher dose rates and for hypofractionated HDR brachytherapy, particularly for tumours or normal tissues which have low α/β ratios. In such cases an SF_{5-7} or an SF assay at the relevant treatment dose rate would be more appropriate.

Normal tissue radiosensitivity assays may become increasingly important. The identification of abnormally radiosensitive patients, such as ataxia telangiectasia heterozygotes, may allow the prospect of relatively safe dose increments to the remainder of the patient population [59, 60]. However, there could also be potential dangers in dose escalation after genetic screening since normal tissue tolerance may be adversely influenced by other factors such as extremes of age, previous surgery and concomitant medical conditions.

Tumour repopulation rates

It is known that many human tumours probably possess cells with clonogenic doubling times of only a few days [61–63]. The short length of time taken to deliver a CLDR treatment thus represents a few doubling times at most, so that any concurrent repopulation is small and insignificant. The same considerations apply in the case of permanent implants utilizing radionuclides with relatively short half-life. In addition, short treatments may also cause increased delays to the cell cycle with enhanced radiosensitivity at the G2/M checkpoint [64].

For FHDR, the overall treatment time will usually be longer than with CLDR, so that repopulation between fractions can be significant. Similarly, for permanent implants with nuclides possessing long half-lives, the amount of repopulation during treatment will also cause a significant proportion of the delivered dose to be wasted [65].

Hypoxia

Tumour radiosensitivity is adversely modified by severe hypoxia [66–71]. There is considerable debate as to whether oxygen is purely dose modifying or if the oxygen enhancement ratio (OER) falls in a predictable way when either dose rate or dose per fraction is reduced [66, 72–74]. There is *in vitro* experimental evidence for a reduction in OER when the dose rate is reduced [75]. In the case of *in vivo* hyperfractionated teletherapy, the OER does not appear to change significantly [76]. This may also hold true for hyperfractionated HDR and CLDR brachytherapy, suggesting that hypoxia may remain a significant cause of radioresistance.

The process of reoxygenation is likely to be time dependent [77] and possibly dependent on tumour shrinkage [78, 79]. Very short radiotherapy schedules will not allow for significant reoxygenation but a relatively protracted teletherapy schedule may well allow for subsequent brachytherapy in more oxic conditions.

If hypoxia persists during radiotherapy, the conditions may be ideal for the administration of hypoxic cell sensitizers (HCS) or bioreductive drugs [68, 80], particularly during hypofractionated HDR or CLDR brachytherapy. The toxicity normally encountered by prolonged exposure to these drugs [81] should not then occur. The availability of commercial microelectrodes [71] and histological methods for the detection of significant hypoxia [72] may provide indications for such intervention. Direct interstitial injection of HCS to tumour tissue is possible in some situations, for example cervix cancer [82–84]. In the case of intraoperative HDR brachytherapy, given in a large single fraction, intravenous or interstitial administration of HCS or the use of O_2 and CO_2 gas mixtures with nicotinamide [76] should enhance the killing of tumour cells.

The reduction of hypoxic radioresistance in brachytherapy has been attempted by the use of neutron emitting Californium-252 sources [85]. Although promising results were reported, the elevated relative biological effectiveness (RBE) in normal tissue, radiation protection problems and high linear energy transfer (LET) carcinogenesis risks preclude its widespread use.

Cell cycle effects

For some cell lines an inverse dose rate effect occurs whereby radiosensitivity increases, rather than decreases, as the dose rate is reduced. The likely explanation is that, at lower dose rates, cells become halted in the relatively radiosensitive G_2 phase of the cell cycle. Thus, under continuous irradiation at a critical dose-rate, an asynchronous population of cells becomes a population of very radiosensitive G_2 cells. At higher dose rates the cells are arrested in the prevailing phase [56]. Tumour sensitivity to CLDR is related to the extent of the G2/M phase block [64]; the lowest dose rate to prevent repopulation appears to be the reciprocal of the mitotic delay per Gy of HDR irradiation [86]. A mathematical model of cell cycle progression during CLDR irradiation has been developed [87].

The role of the inverse dose rate effect in CLDR brachytherapy remains enigmatic. Dose rates of the order of 0.3 Gy h^{-1} are known to induce this effect in HeLa cells *in vitro* [88] but it is not known if the phenomenon occurs *in vivo*. With permanent implants, the dose rate may fall to the

critical value necessary to precipitate the inverse dose rate effect. However, dose rate inhomogeneities throughout a brachytherapy distribution probably ensure that only a fraction of the total number of cells will be simultaneously subjected to that critical dose rate.

Another aspect of cell cycle effects is the possibility that successive fractions may not produce an equal biological effect per fraction [89].

Apoptosis

The control of apoptosis by the p53, bcl-2 and other genes is now better understood, but the contribution of this process to the radiation response *in vivo* remains uncertain [90–95]. There are interesting implications for radiotherapy since p53 mutated cells exhibit enhanced cell survival in hypoxia and reduced apoptotic death following radiation exposure [92, 96]. Although such cells cannot progress beyond the G1 phase in hypoxia [97], they can do so in oxic conditions despite simultaneous irradiation. Mitotic death exceeds apoptotic death after radiation exposure, but the relative apoptotic fraction may increase as dose per fraction or dose rate is reduced [98–100]. The contribution of apoptotic death to tumour control during brachytherapy will thus be greater for hyperfractionated HDR or CLDR at very low dose rates. Ling et al [98] found that the fraction of cells undergoing apoptosis following four daily fractions of 5 Gy was significantly greater than in the case of one fraction of 20 Gy.

Although specific antisense gene therapy can restore the apoptotic potential in patients with lymphoma [101], such approaches have not been tested with radiotherapy. However, in one study, the pre-treatment apoptotic index was found to be predictive of treatment failure in cervix cancer treated by teletherapy and brachytherapy [102].

Biologically effective dose (BED) as applied to brachytherapy

The BED at any particular location is defined in terms of both physical and radiobiological parameters (see Appendices). It is a measure of the total amount of lethal damage sustained by a specified tissue and is protocol dependent. BED is obtained by multiplying the total physical dose by a modifying factor (the relative effectiveness per unit dose, RE). This takes account of the physical aspects of the delivery (*e.g.* dose/fraction, dose rate, dose per pulse, etc.) together with specific radiobiological parameters characteristic of the irradiated tissue. In the BED equations in this article the RE factor is contained within square brackets.

The teletherapy dose within a target volume is relatively homogeneous, thus a single BED figure can be applicable throughout that volume. This is not so for brachytherapy; the dose gradients ensure that either dose or dose rate (and hence, BED) vary with distance from the radiation source(s). Calculations of BED at a few geometrical points may not be sufficient to completely quantify the true biological effect, an aspect frequently overlooked in intercomparisons of brachytherapy treatments. Dose gradient problems can be minimized by a careful selection of the prescription points. For tumours, the likelihood of cell kill rises dramatically in moving inward toward the source(s). Provided the BED at the reference point (which is part of a reference surface) is sufficient to ensure a high tumour cure probability (TCP), any "overkill" within that surface can only be beneficial since the additional dose will help eradicate radioresistant tumour cells. Steel [103] emphasized the rapid fall in cell kill probability from 100% to 0% over a distance of only a few millimetres. Thus, if viable clonogenic cells exist outside the dose reference point, treatment failure is likely. The correct selection of the tumour dose prescription point is therefore of considerable importance.

The influence of dose gradients within normal tissues is less clear. Normal tissue toxicity will depend on a complex interaction between the dose variations within the tissue and the location of potential target cells [104, 105]. Nevertheless, the BED concept can be used effectively to analyse and predict possible late complications. For example, the proposed threshold BED for rectal complications (calculated using an α/β value of 3 Gy) is 90 Gy, and for a 50% morbidity rate is 190 Gy [106].

The "equivalent" BED, within non-uniformly irradiated tissues, may be obtained by considering the integrated cell kill within the volume of interest [107]. A BED value at a single dose reference point can then be multiplied by a multiplying factor (MF) to obtain the "equivalent" BED for the tissue volume enclosed by the surface which contains the dose reference point. The magnitude of MF depends on the treatment prescription at the reference point (*i.e.* dose/fraction for HDR, dose rate for CLDR) and, to a lesser extent, on the tissue radiobiological factors. For a radical brachytherapy treatment, the MF will typically be in the range 1.1–1.30. The MFs for FHDR are summarised in Table 1 using an assumed α value for tumour of 0.35 Gy^{-1}. These factors apply to line and single plane brachytherapy. For volume implants they will be smaller and depend on the prescription method and on the source loading pattern. Multiplying factors are potentially useful in the retrospective intercomparison of clinical brachytherapy treatments, a difficult area due to the various conventions used for treatment prescription [108, 109].

Table 1. Averaged multiplying factors for FHDR ($\alpha/\beta =$ 20 Gy; $\alpha = 0.35\ Gy^{-1}$)

Dose per fraction (Gy)	$N=1$	$N=2$	$N=4$	$N=6$	$N=8$	$N=10$
2	1.72	1.54	1.39	1.32	1.27	1.24
4	1.55	1.39	1.27	1.21	1.18	1.15
6	1.45	1.31	1.21	1.16	1.13	1.11
8	1.38	1.26	1.17	1.13	1.10	1.09
10	1.33	1.22	1.14	1.10	1.08	1.07

The radiobiological features of the main types of brachytherapy

CLDR brachytherapy

Although few clinical trials have examined the consequences of dose rate variations [8–10] CLDR brachytherapy can provide excellent therapeutic results. Three factors, one physical and two radiobiological, can explain the efficacy of CLDR brachytherapy [11]. Tumour overkill occurs very close to the radiation sources while more distant normal structures are preserved—the physical dose effect. Irradiation of normal tissues, at lower dose rates than the tumour, allows additional radiobiological dose sparing. Finally, short treatment durations of a few days limit the repopulation of tumour clonogen during treatment, regardless of cell cycle check point blocks. Despite these advantages, classical CLDR treatments should not be viewed as being invariably the best achievable since physical and radiobiological optimization may allow further improvements.

The relative effectiveness of a single dose delivered at dose rate R over time period T is given by the square bracketed expression in Equation (B1) [32]. For a given dose D, this equation may be rewritten in terms of treatment time, since $R = D/T$. Figure 1 shows how the RE for a late-reacting tissue varies for a single dose of 10 Gy, delivered in times varying from 0.001 h to 1000 h. At low dose rates the RE is ~ 1; at high dose rates it approaches 4.33 when $\alpha/\beta = 3$ Gy and $T_{1/2} = 1.5$ h. This is the same RE as would be expected by delivering an acute single fraction of 10 Gy, derivable from the RE factor in Equation (A1).

The change in RE with T for a constant dose reflects the dose rate effect in the absence of any repopulation. For the single dose of 10 Gy considered here, the major change in RE takes place over the intermediate dose rate range, characterized by treatment times of between 1 and 10 h. This is the region in which medium dose rate brachytherapy treatments operate (treatment times typically in the range 2–3 h for each fraction) and relatively small changes in dose rate, requiring changes in treatment time, have a significant impact on the RE. The importance of treatment time in understanding the dose rate effect is exemplified by Figure 1. Although the changes in RE will be dependent on the precise tissue parameters, the general shape of the curve is always the same, with the largest changes in RE occurring for treatment times of the same order as the half-time for repair of sublethal damage. Clinical trials confirm that small changes in dose rate do influence clinical outcome [8–10].

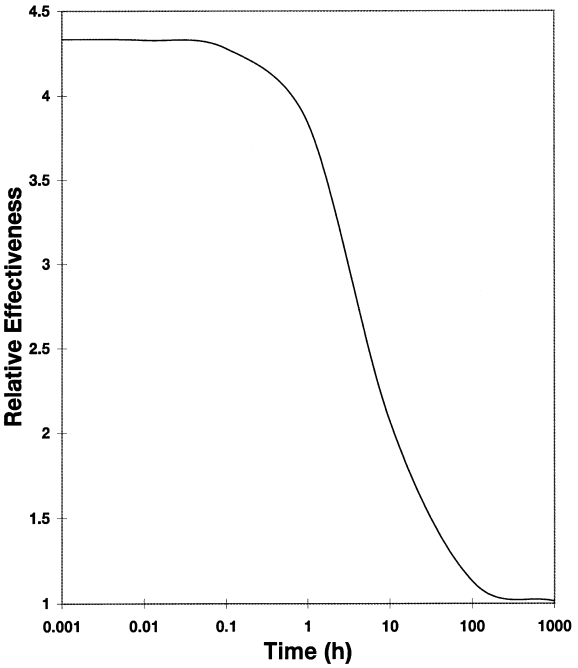

Figure 1. Variation of relative effectiveness (RE) of a single dose of 10 Gy with treatment time (T). Calculated via Equation (B1), with dose rate (R) replaced by ($10/T$) (assumed $\alpha/\beta = 10$ Gy, $T_{1/2} = 1.5$ h).

It is of additional interest to note that the vertical extent of Figure 1 is governed solely by the α/β ratio, the maximum RE (*i.e.* that at very short treatment times) increasing with smaller α/β values and *vice versa*. The lateral spread of the curve is dependent on the recovery half-life. In general terms, the curve is displaced to the left for faster recovery rates and to the right for slower recovery rates. In the case where the recovery kinetics are bi-phasic the individual recovery components will exert most influence when the treatment times are comparable with the half-life of that particular component. Thus, relative to a mono-phasic repair process with the same average repair half-time, the presence of a short half-life component will have the effect of shifting the RE curve slightly to the left at shorter treatment times. The longer half-life component will have the effect of shifting the curve rightward at longer treatment times. A bi-phasic RE curve will thus tend to be more "spread out" than its mono-phasic equivalent, the relative partitioning between the short- and long-lived components determining the overall shape of the composite curve. RE variations for

specific combinations of multiphasic recovery parameters may be determined using the square bracketed term in Equation (B4).

Fractionated high dose rate brachytherapy

HDR techniques typically involve dose rates such that each fraction is normally completed in less than 10 min. For such short exposure times there is no dose rate effect *per se*, but correction may be required for longer times, particularly if stepping sources are used [110]. DNA repair occurs only between successive fractions and, provided the gaps are long enough to ensure complete repair, the repair rate is irrelevant. This explains why LQ equations, for well spaced (>12 h) fractionated treatments, do not normally require a correction for incomplete repair.

Although FHDR was introduced over 30 years ago, the radiobiological comparisons between FHDR and CLDR continue to be debated [22, 30, 111, 112]. Provided sufficient fractions are used, FHDR can safely replace CLDR and produce similar tumour and late tissue effects [21, 32, 113]. However, there are circumstances in which the required number of fractions can be made small without significant loss of the therapeutic ratio (TR), as discussed below.

The radiobiological correspondence between dose rate and fractionation effects: implications for FHDR

The biological consequences of changing the dose per fraction in a teletherapy treatment may be emulated by changing the dose rate in a CLDR treatment [32, 43]. The changes in cell survival caused by increased fractionation or reduced dose rate for two tissue types are illustrated in Figures 2–5. In each case the radiobiological sparing is dependent on controllable factors (dose per fraction or dose rate), and on the shape of the underlying cell survival curve, characterized by the α/β value. For a change in dose rate, the sparing is additionally dependent on μ.

It is the *time dependent* β-damage alone which changes as dose rate is altered; the α-damage is unaffected by changing dose rate and is related only to the total dose [32]. The dose rate phenomenon is thus not determined by the dose rate *per se*; it is the dose rate *and* the irradiation time which together determine the magnitude of dose rate effects. Radiobiology text books often omit this essential fact.

Figure 6 shows how the iso-effect dose/fraction for tumour and normal tissue varies with FHDR as fraction number is varied. The reference CLDR regime in this case is 40 Gy/48 h, and the assumed radiobiological parameters are $\alpha/\beta = 10$ Gy, $T_{1/2} =$ 1.5 h (for a tumour) and $\alpha/\beta = 3$ Gy and $T_{1/2} =$ 1.5 h (for a late-reacting normal tissue). The iso-effect doses have been calculated by equating Equations (A1) and (B3). The fact that the two curves are not coincident is a reflection of the differing fractionation sensitivities of the two tissues. The point of equivalence, at which the effects of the FHDR and CLDR treatments are identical for both groups of tissues, is determined from the intersection point of the two curves. For the assumed CLDR regime and the parameters used this occurs at approximately 11 fractions. Where tumour and normal tissue recovery constants are identical (as assumed here), the same result can be obtained by application of the general Liversage equation [21]. FHDR using less than 11 fractions will have a lower TR relative to the CLDR. Conversely, the use of over 11 fractions is likely to improve the TR, but may be impractical. The results of following this same procedure with a tumour recovery half-life of 0.5 h, the other parameters remaining unchanged, are shown in Figure 7. In this case the intersection occurs at around four

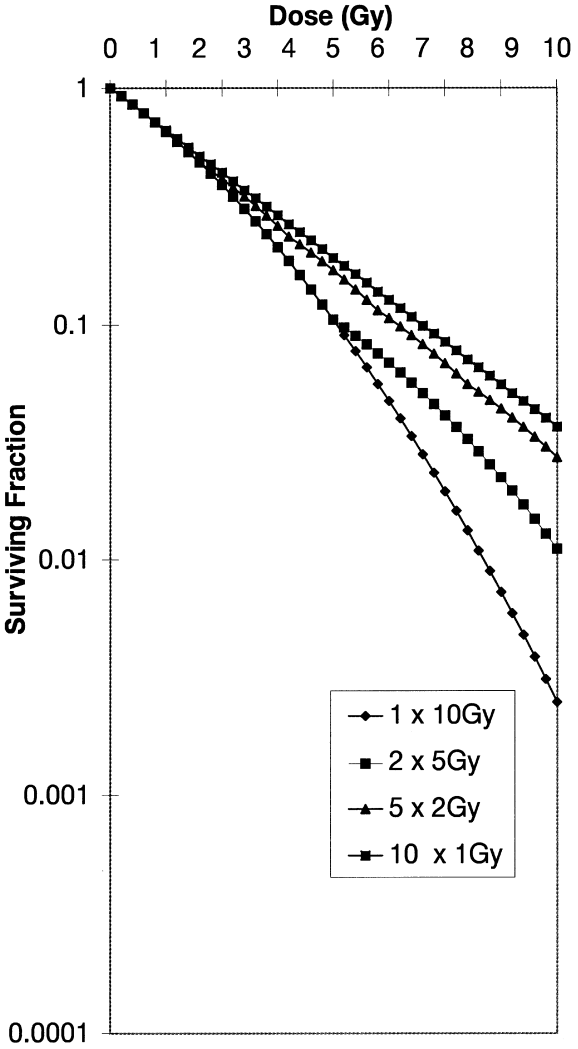

Figure 2. Effect of HDR fractionation on a tumour (assumed $\alpha/\beta = 10$ Gy).

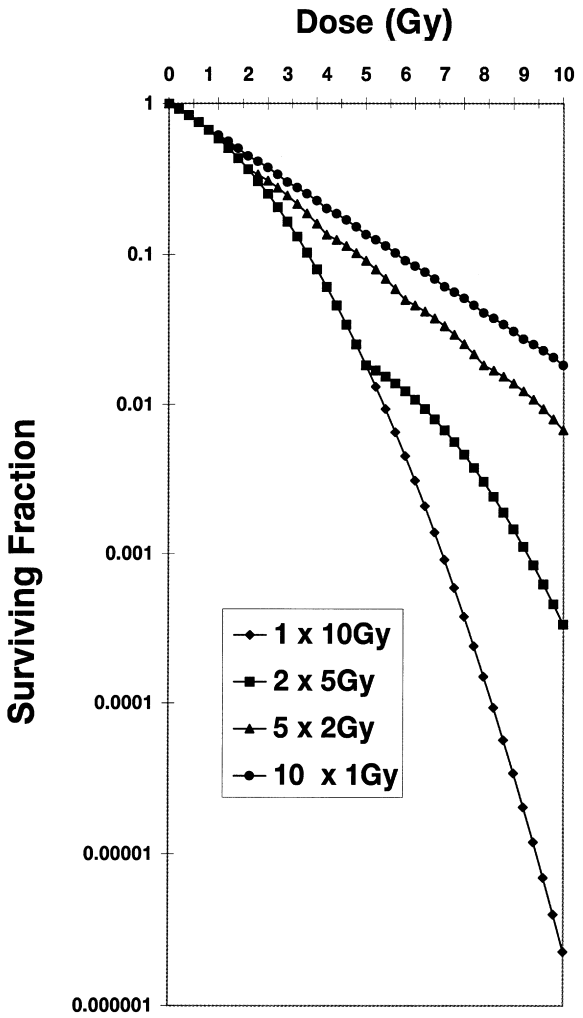

Figure 3. Effect of HDR fractionation on a late-reacting normal tissue (assumed $\alpha/\beta = 3$ Gy).

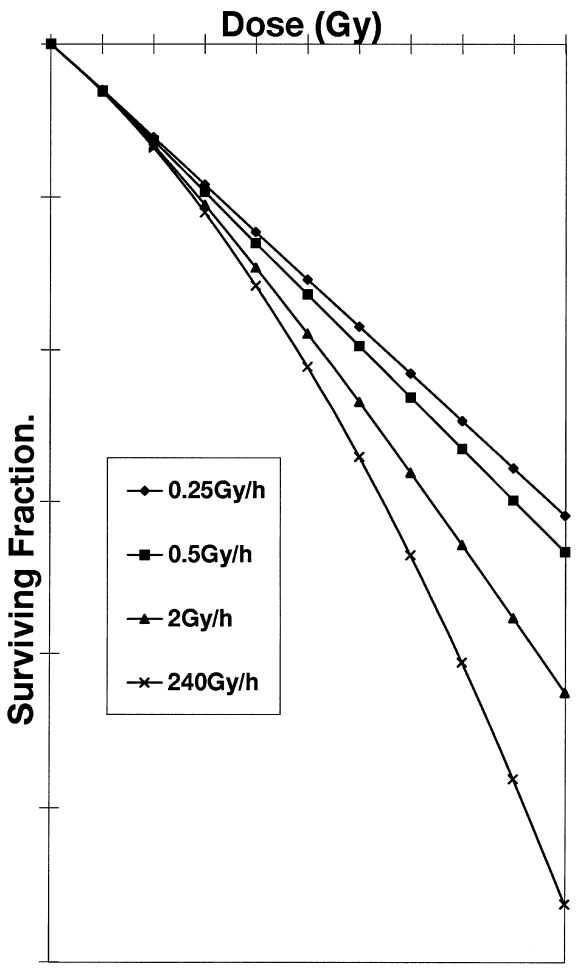

Figure 4. Effect of changing dose rate on a tumour (assumed $\alpha/\beta = 10$ Gy, $\mu = 0.5\ h^{-1}$).

fractions and fewer FHDR fractions are required to achieve equivalence with the original CLDR regime.

A further determinant of the fraction number is the extent of sparing of normal tissue by geometric factors [114–116]. Improved applicator placement with FHDR provides reproducible additional geometrical sparing of normal tissues, especially in gynaecological applications where displacement of paravaginal (but not parauterine) tissues can be achieved. Figure 8 is identical to Figure 6 (*i.e.* with identical half-lives for tumour and normal tissue), but with 20% normal tissue sparing. That is the total dose *and dose per fraction* to the normal tissue are each 20% less at FHDR than those received by the tumour. The modest additional geometrical sparing is seen to be very effective; the intersection point has been reduced from 11 to 5 fractions. The benefits of combining 20% additional normal tissue sparing with a favourable differential in the recovery half-lives is illustrated in Figure 9. This is the same as Figure 7, but with 20% sparing. In this case the intersection point occurs at one fraction. [114, 117–119]. The principal conclusion is that additional geometrical sparing of normal tissues using FHDR may easily cancel out the potential radiobiological disadvantages [120], the treatment being more "forgiving" of adverse radiobiological parameters.

There is another reason why hypofractionated FHDR may have advantages in certain circumstances [121]. The dose/fraction, like the total dose, varies continuously with distance from the source(s) and therefore the RE also varies with distance. If the physical dose decreases with increasing distance then, irrespective of the precise physics of the dose fall-off, the radiobiological dose gradient will always be steeper than the physical dose gradient.

The nature of this effect is summarised in Figure 10. If the BED values are matched at a particular geometrical location (point M, part of a three-dimensional iso-effect surface), then the FHDR and CLDR dose gradients are different at points closer to, or further from, the source. The difference becomes larger as the number of FHDR fractions is reduced, the FHDR producing more biological damage than CLDR at locations within the reference surface and increasingly less damage

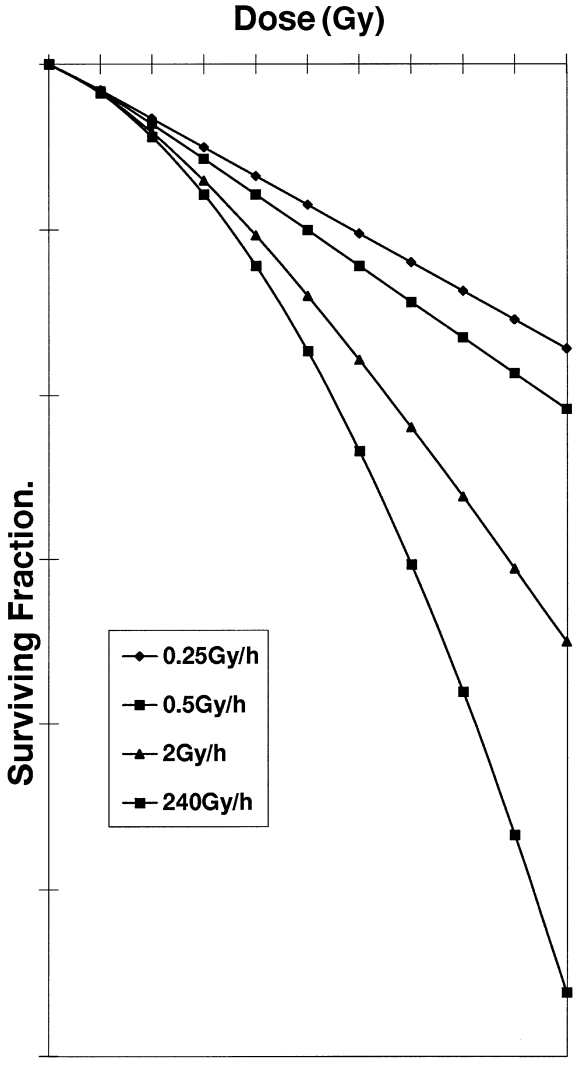

Figure 5. Effect of changing dose rate on a late-reacting normal tissue (assumed $\alpha/\beta = 3$ Gy, $\mu = 0.5$ h^{-1}).

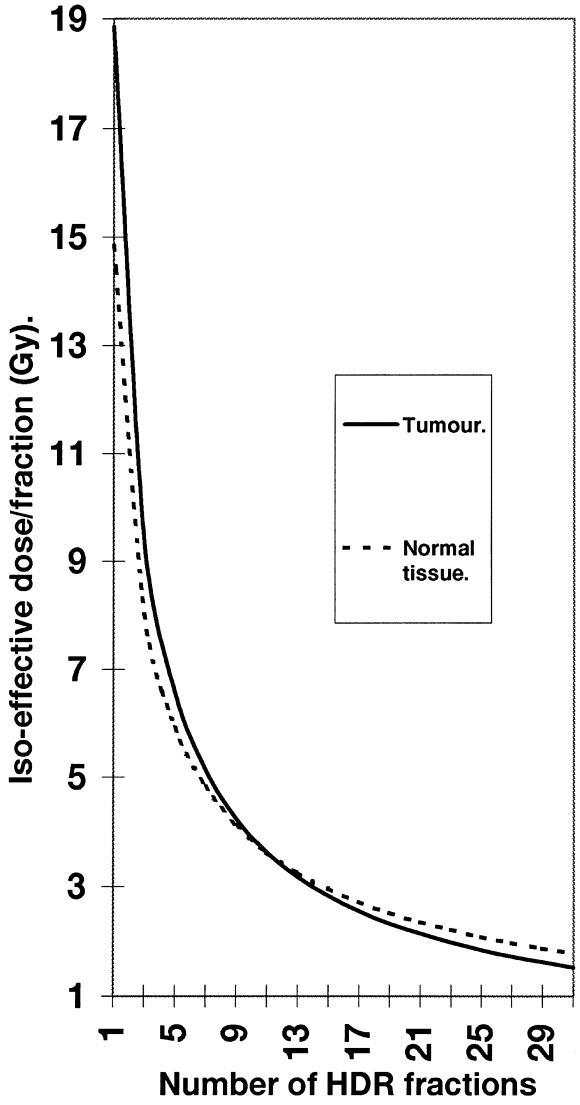

Figure 6. Variation of iso-effective dose for tumour and late-reacting normal tissue with changing HDR fraction number. Matched to a CLDR regime of 40 Gy/48 h. Tumour and late-normal doses identical (assumed parameters: $(\alpha/\beta)_{tum} = 10$ Gy, $(\alpha/\beta)_{late} = 3$ Gy, $(T_{1/2})_{tum} = 1.5$ h, $(T_{1/2})_{late} = 1.5$ h).

at locations without. Assuming that most of the tumour lies inside the reference surface, and most critical structures outside, this phenomenon predicts an enhanced TR for hypofractionated HDR treatment.

Although this effect is easy to understand in terms of point-source geometry, in the case of multiple catheters and source/dwell positions it is more difficult to predict the biological consequences, but three-dimensional radiobiological treatment planning will allow further exploration of these relationships [107]. Since each iso-effect surface encloses a specific tissue volume, such concepts may in future provide a method for quantifying radiobiological volume effects in brachytherapy, particularly if reliable normal tissue complication functions are included.

The radiobiological optimization of fractionated HDR brachytherapy

Individual optimization of fractionation can be studied for a given set of normal tissue and tumour parameters by calculus methods [122]. The optimum dose per fraction may be found as the solution for d of Equation (F3), where f is the mean interfraction interval. Equation (F3) assumes that the tumour and critical normal tissue each receive the same dose and dose/fraction.

When normal tissue sparing is achievable (as in most brachytherapy applications), the equation is modified to Equation (F4), where z is now the tumour dose and d the normal tissue dose per fraction. Factor $g\ (=d/z)$ is the geometrical sparing between tumour and normal tissue. Normal tissues sparing helps in allowing FHDR to be performed with relatively few fractions [114, 118, 119] and Equation (F4) allows examination of the interplay between the various parameters.

For example, Figure 11 shows values of optimum dose/fraction for tumours with various dose

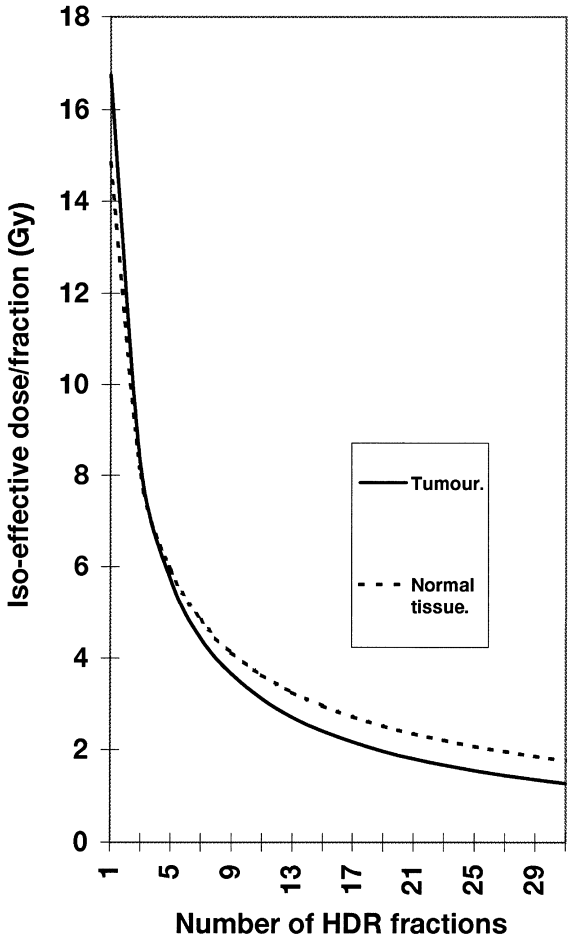

Figure 7. As for Figure 6, but with $(T_{1/2})_{tum} = 0.5$ h.

equivalents of daily repopulation rates (K), treated thrice weekly. When K is 0.6 Gy day^{-1} (typical of some squamous cell carcinomas [33]) and with $g = 0.8$ (easily achievable in most gynaecological applications) the optimal fraction size for the tumour is in the range 3–8 Gy. This range corresponds with those found acceptable in clinical practice [23, 109, 119] and has been obtained by non-comparative application of LQ-based methodology, *i.e.* without reference to classical CLDR prescriptions.

Where geometrical sparing cannot be achieved (*e.g.* in central nervous system brachytherapy), the use of smaller fraction sizes is indicated. If tumour repopulation is a potential problem and if brachytherapy catheters can only remain in place for relatively few days, then the interfraction interval (f) should be kept as short as possible [79].

Pulsed brachytherapy (PB)

PB involves the delivery of a large number of radiation pulses over a time period similar to that used in CLDR. Pulse durations are typically of the order of 10–20 min, with interpulse intervals of up to a few hours. The nominal dose rate within any one pulse may be up to 12 Gy h^{-1} and, as with

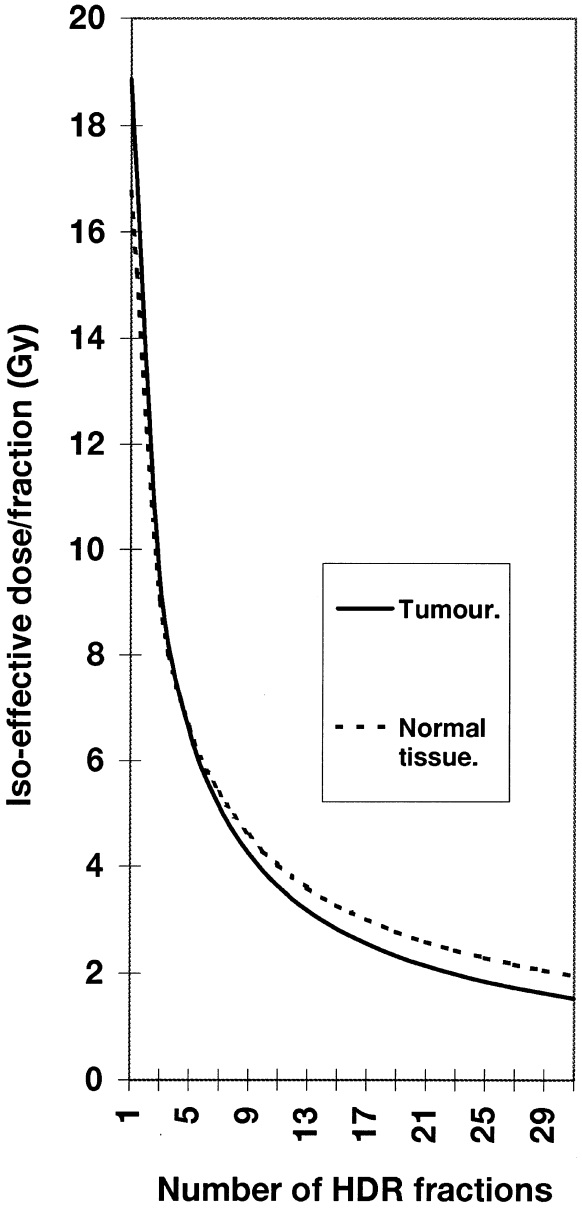

Figure 8. As for Figure 6, but with 20% geometrical sparing for normal tissues at HDR.

FHDR, will be much higher in close proximity to source dwell positions [123]. PB is designed to provide the radioprotective benefits of FHDR for hospital staff, whilst retaining the clinical advantages of delivering the entire dose within a few days as in CLDR.

The potential of PB to mimic the radiobiological aspects of CLDR is dependent on the interplay between the pulse repetition frequency and the interpulse interval. Use of the LQ model indicates that, for pulses delivered at hourly intervals, there should be no significant differences between PB and CLDR [54, 124–126]. This appears to be reasonably true irrespective of the repair rate. However, if the number of pulses is decreased, thereby increasing both the interpulse interval and the dose per pulse, there may be a significant increase in the complication risk for a sub-set of

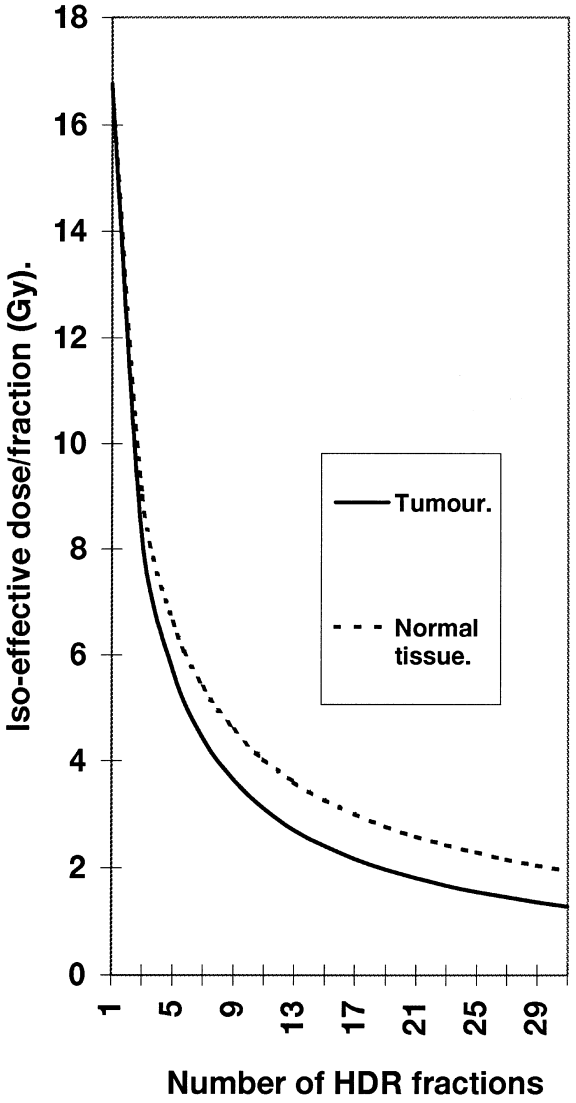

Figure 9. As for Figure 7, but with 20% geometrical sparing for normal tissues at HDR.

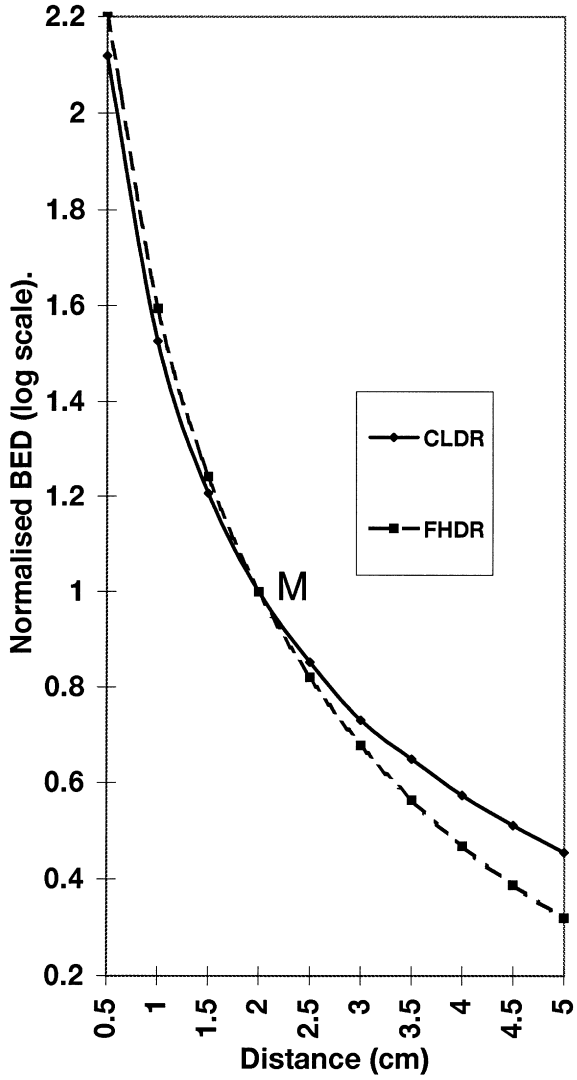

Figure 10. Intercomparison of iso-effect lines for CLDR and FHDR.

cases [127]. This could be offset by reducing the total dose, but only by concurrently decreasing the tumour cure probability, *i.e.* the therapeutic index relative to CLDR would be reduced.

Visser et al have examined whether theoretically it might be possible to allow longer intervals between fractions if the overall time of the PB is longer than that of the CLDR which is being replaced [128]. The indications are that, although intensive, fractionation is always the safest option, provided there is a small modification to the total dose with PB, intervals of as long as 3 h may be adequate if PB is used only as a component of radical radiotherapy. Logistic benefits would accrue if interfraction intervals could be extended to 3 h, but there are risks of adverse effects.

Modelling studies show that any tissue with a substantial fast-repair component (*i.e.* half-life less than about 0.5 h) is likely to be more damaged by PB than by CLDR [53, 123, 129, 130–132]. The effect becomes more significant as the half-life begins to approximate to the length of the pulse duration, the PB then behaving more like FHDR than CLDR [123]. However, if there are longer half-life repair components present, the overall effect is to some extent diluted and the practical way to minimize such untoward effects is to keep the dose per pulse small, ideally at around 0.5 Gy.

The PB equations for mono- and bi-exponential repair kinetics are given in Appendix C. The mathematics appears daunting, but it is useful to note that the calculation of BED where multiphasic recovery exists can be accomplished using mono-phasic equations by following three logical steps, as described by Haustermans et al [131].

(i) Using the specific time/pulse configuration, calculate the RE value for each half-time component using the appropriate mono-phasic equations [124, 133].
(ii) Calculate the "effective" RE for the multiphasic case from a weighted summation of the individual RE values, the weighting factors being the

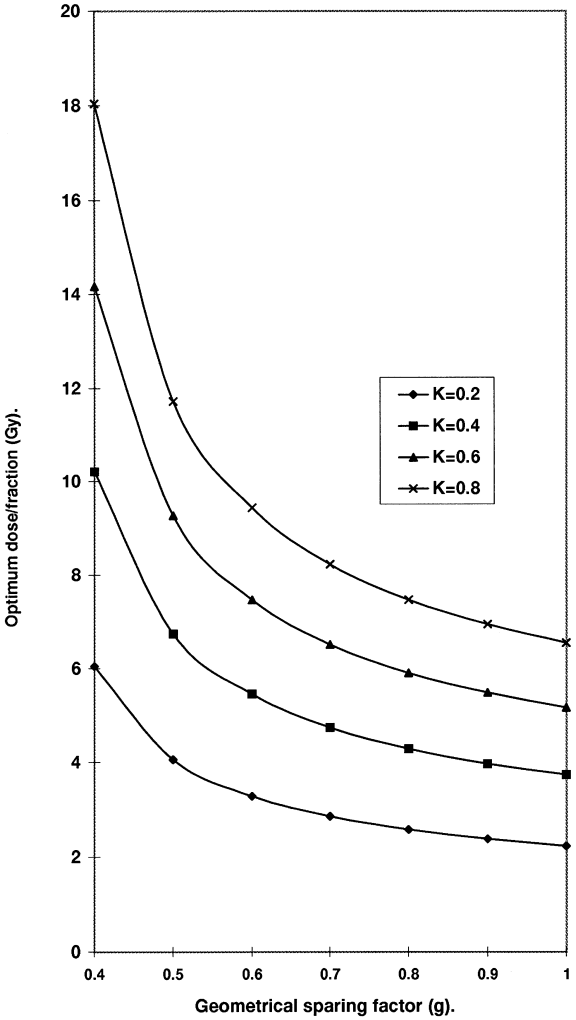

Figure 11. Variation of optimum dose/fraction with geometrical sparing factor (g). Calculated using Equation (F4) (assumed $(\alpha/\beta)_{tumour} = 10$ Gy; $(\alpha/\beta)_{late} = 3$ Gy. Thrice-weekly treatment is assumed, *i.e.* $f = 7/3$ days).

fractional contribution of each assumed recovery half-life.

(iii) The BED for multiphasic recovery is obtained by multiplying the total dose by the effective RE.

(The attractiveness of this simple method is that it may also be generally applied to CLDR and HDR. The PB equations in step (i) simply being replaced by those relevant to calculating mono-phasic REs for the alternative modalities).

As discussed earlier, the geometrical form of a brachytherapy treatment is always very relevant and will also have a bearing in PB treatments. Indeed, some of the potential difficulties identified from animal experiments may be a consequence of not maintaining exactly the same physical dose distribution in the various arms which are being compared [146, 147]. Nevertheless, with a large number of variable physical parameters and a number of (largely unquantified) radiobiological influences, it is more difficult to predict outcomes with this modality [54, 125, 133, 134]. Because the clinical introduction of pulsed brachytherapy techniques has been based on theoretical assumptions, the modelling predictions may require careful empirical modification in the clinic. The results from the departments which pioneer PB are thus awaited with interest [135, 136].

Permanent implants

Several nuclides are used for permanent implants, *e.g.* gold-198 ($T_{1/2} = 2.7$ days), iodine-125 ($T_{1/2} = 60$ days) and palladium-103 ($T_{1/2} = 17$ days). Ytterbium-169 ($T_{1/2} = 32$ days) has also been suggested [137, 138]. The use of decaying radionuclides complicates the usual dose rate effect because the initial dose rate is governed by both the dose which is to be delivered and the nuclide half-life. For example, a permanent implant delivering 70 Gy with gold-198 requires an initial dose rate of 0.75 Gy h^{-1}, whereas the much higher dose of 160 Gy which is often specified for ^{125}I requires an initial dose-rate of only 0.08 Gy h^{-1}. The time taken to deliver the doses varies greatly; with gold-198, half of any prescribed dose is delivered in less than 3 days; with iodine-125 it takes 60 days to deliver half the dose. Thus ^{125}I implants in particular would appear to be contraindicated for tumours with short clonogen doubling times (*e.g.* squamous cell carcinomas), being more appropriate for slow growing neoplasms (*e.g.* prostate cancer).

The dose rate will eventually fall below that required to prevent clonogenic proliferation [65, 139, 140], hence giving rise to the concept of "wasted dose" associated with permanent brachytherapy implants. The relevant equations are given in Appendix D. Implants utilizing longer-lived nuclides are more likely to involve a higher fraction of wasted dose, but the amount may be reduced by on-going tumour shrinkage. If shrinkage begins soon after the application of a permanent brachytherapy implant then the dose rates received by individual clusters of cells, because they can move closer to the sources, may decrease with time at a rate which is slower than that of the decay half-life [78]. This leads to substantial modification of the relevant BED equations, as is outlined in Appendix E. The implications are that nuclide $T_{1/2}$s could be selected to match the ratio of the tumour shrinkage and repopulation rates and there is already experimental evidence that the choice of radionuclide may influence tumour control [7]. Furthermore, from clinical observations, it has been demonstrated that a rapid tumour shrinkage rate may increase normal tissue toxicity [141].

Combined teletherapy and brachytherapy

Combination treatments confer practical advantages, such as reducing the number of HDR brachytherapy fractions required. If the teletherapy and brachytherapy BED values are summated to within a tolerance value, the teletherapy provides a radiobiological "dilutional" effect which can offset suboptimal features of brachytherapy: the normal tissues are protected by the homogenous dose of hyperfractionated teletherapy and by the "small volume" effect of brachytherapy. These considerations apply irrespective of whether the brachytherapy component is delivered as CLDR, FHDR, PB or permanent implant [128].

Rarely, it may be necessary to treat by a combination of CLDR and HDR brachytherapy, for example when CLDR treatment is not well tolerated and has to be discontinued. The remainder of the treatment can then be given by HDR, the dose fractionation being selected to maintain the originally prescribed iso-effect by LQ modelling [142–145].

Tumour volume changes

The decision as to whether brachytherapy is best delivered before, after or during the teletherapy will depend on the tumour repopulation and shrinkage rates [38, 142]. Teletherapy is frequently given first to large treatment volumes which include areas of potential microscopic tumour infiltration and nodal metastases [142]. The primary tumour then shrinks and brachytherapy is later given to a smaller tumour, which results in an increased tumour dose providing the brachytherapy is prescribed at a standard distance.

The tumour BED will increase only if the tumour cell doubling time is sufficiently long relative to the tumour regression rate [79]. An adverse situation can occur when the tumour cell doubling time is short and the regression rate is slow: additional treatment modalities such as chemotherapy are then indicated in order to minimize repopulation while allowing tumour shrinkage to continue and then using brachytherapy when the tumour is sufficiently small [142, 143].

Further allowance for the geometric conditions of treatment, *e.g.* in the placement of line sources in intralumenal therapy, show that poor source positioning relative to the tumour centre can completely negate the potentially beneficial effect of tumour shrinkage [39], such that brachytherapy should be used during teletherapy. Similarly, the optimal interfraction interval for HDR has been shown to be related to the ratio of the regression rate and the tumour effective doubling time. In the majority of clinical situations, modelling studies predict that the interfraction interval should be kept reasonably short [79].

For cervix cancer, steady state exponential tumour volume regression commences during the first week of teletherapy [143]. If the repopulation rate does increase at around 21–28 days, due to changes in cell loss factor or growth factor [146], then brachytherapy should ideally be performed at around this time when the dose benefits of tumour shrinkage will not as yet be opposed by that effect. Gene therapy protocols offer a future prospect for prevention of accelerated repopulation, which could then provide greater scope for using brachytherapy to very small residual tumour volumes at longer time intervals after teletherapy.

Conclusion

At the experimental level there are increasing reports of reproducible animal models which may be used to investigate the biological basis of brachytherapy and to help confirm theoretical predictions. This is a timely development since brachytherapy has evolved largely empirically and a firmer understanding of the underlying scientific principles is required if best use is to be made of the potentially wide range of techniques now available.

Whereas relevant clinical deductions can be made by mathematical modelling, the current inability of laboratory experiments to provide quick and reliable estimates of radiobiological parameters for individual patients precludes further progress [147]. Further refinement in modelling may help make brachytherapy more effective through optimization of treatment delivery [96, 148]. This process will likely be aided by the development of new radiobiological software, utilizing a combination of cell killing and integrated response models. Improved imaging techniques, together with accurate control and manipulation of source dwell positions, will provide the ability to shape radiation dose distributions to fit a wider range of tumours and at previously inaccessible anatomical sites. Increasing use of predictive radiobiological assays and knowledge of the parameter variations in specific tumour sub-types should improve selection of the patients who can most benefit from existing treatment schedules, and could allow more innovative approaches in individual cases. Eventually, genetic assays might provide more reliable predictive data [92, 96, 149, 150].

With an increased scientific understanding and technological capability, the prospect of optimal individualized therapy, rather than standard treatment prescriptions for all patients, should emerge. That will allow greater utilization of the concepts discussed in this article.

Acknowledgments

We would like to thank Drs Jack Fowler, Anthony Howes, Bill Millar and Charles Deehan for their interest and encouragement. RGD wishes to thank Drs Clifton Ling and Lowell Anderson (New York) for many stimulating discussions.

References

1. Ling CC, Fuks Z. Conformal radiation treatment: A critical appraisal. Eur J Cancer 1995; 31(A):799–803.
2. Wells RL, Bedford JS. Dose-rate effects in mammalian cells. IV: Repairable and non-repairable damage in non-cycling C3H $10T_{1/2}$ cells. Radiat Res 1983;94:105–34.
3. Steel GG, Down JD, Peacock JH, Stephens TC. Dose-rate effects and the repair of radiation damage. Radiother Oncol 1986;5:321–31.
4. Steel GG, Deacon JM, Duchesne GM, et al. The dose-rate effect in human tumour cells. Radiother Oncol 1987;9:299–310.
5. Wilkinson JM, Hendry JH, Hunter RD. Dose-rate considerations in the introduction of low dose-rate afterloading intracavitary techniques for radiotherapy. Br J Radiol 1980;53:890–3.
6. Nath R, Martin DF, Park CH, et al. Development of a 241-Am applicator for continuous low dose rate irradiation of the rat sarcoma BA 1112. Int J Radiat Oncol Biol Phys 1987;13:1883–92.
7. Nag S, Ribovitch M, Cai JZ, Wientjes MG. Palladium-103 *vs* iodine-125 brachytherapy in the Dunning-PAP rat prostate tumor. Endocuriether Hyperther Oncol 1996;12:119–24.
8. Mazeron JJ, Simon JM, Crook JM, Calitchi E, et al. Influence of dose rate on local control of breast carcinoma treated by external beam irradiation plus iridium-192 implant. Int J Radiat Oncol Biol Phys 1991;21:1173–7.
9. Mazeron JJ, Simon JM, Le Péchoux C, Crook JM, et al. Effect of dose rate on local control and complications in definitive irradiation of T1–2 squamous cell carcinomas of mobile tongue and floor of mouth with interstitial iridium-192. Radiother Oncol 1991;21:39–47.
10. Lambin P, Gerbaulet A, Kramar A, Scalliet P, et al. Phase III trial comparing two low dose rates in brachytherapy of cervix carcinoma: report at two years. Int J Radiat Oncol Biol Phys 1993;25:405–12.
11. Scalliet P, Gerbaulet A, Dubray R. HDR *versus* LDR gynecological brachytherapy revisited. Radiother Oncol 1993;28:118–26.
12. Stuben G, Van Der Kogel AJ, Van Der Schueren E. Biological equivalence of low dose rate to multifractionated high dose rate irradiations: Investigations in mouse lip mucosa. Radiother Oncol 1997; 42:189–96.
13. Pop LAM, Van Der Plas M, Skwarchuk MW, Hanssen AEJ, Van Der Kogel AJ. High dose rate (HDR) and low dose rate (LDR) interstitial irradiation (IRT) of the rat spinal cord. Radiother Oncol 1997;42:59–67.
14. White JR, Armour EP, Armin A-R, Dewitt CC, Corry PM, Martinez A. Reproducible rat model for comparing late rectal toxicity from different brachytherapy techniques. Int J Radiat Oncol Biol Phys 1997;37:1155–61.
15. Henschke UK. "Afterloading" applicators for radiation therapy of carcinoma of the uterus. Radiology 1960;74:834.
16. Walstam R. Remotely controlled afterloading radiotherapy apparatus (a preliminary report). Phys Med Biol 1962;7:225–8.
17. O'Connell D, Howard N, Ramsey NW, Liversage WE. The treatment of uterine carcinoma using the Cathetron. Part 1: Technique. Br J Radiol 1967;40:882–7.
18. Joslin CAF, O'Connell D, Howard N. The treatment of uterine carcinoma using the Cathetron. Part III: Clinical considerations and preliminary reports on treatment results. Br J Radiol 1967;40:895–904.
19. Liversage WE. The application of cell survival theory to high dose-rate intracavitary therapy. Br J Radiol 1966;39:338–49.
20. Liversage WE. A general formula for equating protracted and acute regimes of radiation. Br J Radiol 1969;42:432–40.
21. Hammer J, Seewald DH, Track C, Zoidl JP, et al. Breast cancer: primary treatment with external beam radiation therapy and high dose rate iridium implantation. Radiology 1994;193:573–7.
22. Liversage WE. A comparison of the predictions of the CRE, TDF and Liversage formulae with clinical experience. In: Bates TD, Berry RJ, editors. High dose-rate afterloading in the treatment of cancer of the uterus, Report 17. London: British Institute of Radiology, 1980:182–9.
23. Liversage WE, Dale RG. Dose–time relationships in irradiated weevils and their relevance to mammalian systems. Current Topics Radiat Res Q 1978;13:97–187.
24. Wilson CW. Radium therapy: Its physical aspects and extensions with radioactive isotopes. London: Balliere, Tindall and Cox, 1956.
25. Jones B, Tan LT, Freestone G, Bleasdale C, et al. Non-uniform dwell times in line source high dose rate brachytherapy: physical and radiobiological considerations. Br J Radiol 1994;67:1231–7.
26. Anderson LL. A "natural" volume–dose histogram for brachytherapy. Med Phys 1986;13:898–903.
27. Ling CC, Roy J, Sahoo N, Wallner K, Anderson LL. Quantifying the effect of dose inhomogeneity in brachytherapy: application to permanent prostatic implants with ^{125}I seeds. Int J Radiat Oncol Biol Phys 1994;28:971–8.
28. Thomadsen BR, Houdek PV, Van Der Laarse R, Edmundson GK, et al. Treatment planning and optimization. In: Nag S, editor. HDR brachytherapy: A textbook. Amonk, NY: Futura Publishing Company, 1994:79–145.
29. Hunter RD. Editorial: Intracavitary systems. Radiother Oncol 1996;39:95–6.
30. Trott NG, editor. Radionuclides in brachytherapy: radium and after. British Journal of Radiology Suppl 21. London: British Institute of Radiology, 1987.
31. Barendsen GW. Dose fractionation, dose-rate and iso-effect relationships for normal tissue responses. Int J Radiat Oncol Biol Phys 1982;8:1981–97.
32. Dale RG. The application of the linear quadratic dose–effect equation to fractionated and protracted radiotherapy. Br J Radiol 1985;58:515–28.
33. Fowler JF. The linear-quadratic formula and progress in fractionation. Br J Radiol 1989;62:679–94.
34. Thames HD. An "incomplete-repair" model for survival after fractionated and continuous irradiations. Int J Radiat Biol 1985;47:319–39.

35. Thames HD. Repair kinetics in tissues: Alternative models. Radiother Oncol 1989;14:321–7.
36. Nilsson P, Thames HD, Joiner MC. A generalised formulation of the incomplete-repair model for cell survival and tissue response to fractionated and low dose rate irradiation. Int J Radiat Oncol Biol Phys 1990;57:127–42.
37. Millar WT, Canney PA. Derivation and application of equations describing the effects of fractionated protracted irradiation, based on multiple and incomplete-repair processes. Part 1: Derivation of equations. Int J Radiat Biol 1993;64:275–91.
38. Jones B, Dale RG, Bleasdale C, Tan LT, Davies MA. Mathematical model of intraluminal and intracavitary brachytherapy. Br J Radiol 1994;67:805–12.
39. Jones B, Bleasdale C, Tan LT, Shaw JE, et al. The achievement of isoeffective bronchial mucosal dose during endobronchial brachytherapy. Int J Radiat Oncol Biol Phys 1995;33:195–9.
40. Sethi T, Ash DV, Flynn A, Workman G. Replacement of hairpin and loop implants by optimised straight line sources. Radiother Oncol 1996;39:117–21.
41. Joiner MC. The dependence of radiation response on dose per fraction. In: McNally NJ, editor. The scientific basis of modern radiotherapy, BIR Report 19. London: British Institute of Radiology, 1989:20–6.
42. Turesson I, Joiner MC. Clinical evidence of hypersensitivity to low doses in radiotherapy. Radiother Oncol 1996;40:1–3.
43. Fowler JF. Dose-rate effects in normal tissues. In: Mould RF, editor. Brachytherapy 2, Proceedings of the 5th International Selectron Meeting, 1988. Leersum, The Netherlands: Nucletron International BV, 1989:26–40.
44. Badie C, Alsbeih G, Reydellet I, Arlett C, Fertil B, Malaise EP. Dose-rate effects on the survival of irradiated hypersensitive and normal human fibroblasts. Int J Radiat Biol 1996;70:563–70.
45. Thames HD, Hendry JH. Fractionation in radiotherapy. London: Taylor and Francis, 1987.
46. Thames HD, Bentzen SM, Turesson I, Overgaard M, et al. Fractionation parameters for human tissues and tumors. Int J Radiat Biol 1989;56:701–10.
47. Joiner MC, van der Kogel AJ. The linear-quadratic approach to fractionation and calculation of isoeffect relationships. In: Steel GG, editor. Basic clinical radiobiology. London: Edward Arnold, 1993:106–122.
48. Liversage WE. The rate of decay of the dose equivalent of radiation induced sub-lethal damage. Cell Tissue Kinetics 1969;2:269–76.
49. Curtis SB. Lethal and potentially lethal lesions induced by radiation—a unified repair model. Radiation Res 1986;106:252–70.
50. Ang KK, Jiang GL, Guttenberger R, Thames HD, et al. Impact of spinal cord repair kinetics on the practice of altered fractionation schedules. Radiother Oncol 1992;25:287–94.
51. Van Rongen E, Thames HD, Travis EL. Recovery from radiation damage in mouse lung: Interpretation in terms of two rates of repair. Radiat Res. 1993;133:225–33.
52. Van Den Aardweg GJMJ, Hopewell JW. The kinetics of repair for sublethal radiation-induced damage in the pig epidermis: an interpretation based on a fast and slow component of repair. Radiother Oncol 1992;23:94–104.
53. Millar WT, Van Den Aardweg GJMJ, Hopewell JW, Canney PA. Repair kinetics in pig epidermis: an analysis based on two separate rates of repair. Int J Radiat Biol 1996;69:123–40.
54. Millar WT, Hendry JH, Canney PA. The influence of the number of fractions and bi-exponential repair kinetics on biological equivalence in pulsed brachytherapy. Br J Radiol 1996;69:457–68.
55. Steel GG, Kelland LR, Peacock JH. The radiobiological basis for low dose-rate radiotherapy. In: Mould RF, editor. Brachytherapy 2, Proceedings of the 5th International Selectron Meeting, 1988. Leersum, The Netherlands: Nucletron International BV, 1989:15–25.
56. Hall EJ. Radiobiology for the radiologist (4th edn). Philadelphia: Lippincott, 1994.
57. West CML. Invited review: Intrinsic radiosensitivity as a predictor of patient response to radiotherapy. Br J Radiol 1995;68:827–37.
58. Withers HR, Peters LJ, Taylor JMG, Owen JB, et al. Local control of carcinoma of the tonsil by radiation therapy: an analysis of patterns of fractionation in nine institutions. Int J Radiat Oncol Biol Phys 1995;33:549–62.
59. Burnett NG, Wurm R, Nyman J, Peacock JH. Normal tissue radiosensitivity—how important is it? Clin Oncol 1996;8:25–34.
60. Tucker SL, Geara FB, Peters LJ, Brock WA. How much could the radiotherapy dose be altered for individual patients based on a predictive assay of normal tissue radiosensitivity? Radiother Oncol 1996;38:103–13.
61. Wilson GD. Limitations of the bromodeoxyuridine technique for measurement of tumour proliferation. In: Beck-Bornholdt HP, editor. Current topics in clinical radiobiology of tumours. Berlin: Springer-Verlag, 1993:27–44.
62. Hendry JH, Bentzen S, Dale RG, Fowler JF, et al. A modelled comparison of the effects of using different ways to compensate for missed treatment days in radiotherapy. Clin Oncol 1996;8:297–307.
63. Tsang RW, Fyles AW, Kirkbride P, Levin W, et al. Proliferation measurements with flow cytometry T_{pot} in cancer of the uterine cervix: correlation between two laboratories and preliminary clinical results. Int J Radiat Oncol Biol Phys 1995;32:1319–29.
64. Knox SJ, Sutherland W, Goris MC. Correlation of tumour sensitivity to low dose rate irradiation G2/M phase block and other radiobiological parameters. Radiat Res 1993;135:24–31.
65. Dale RG. Radiobiological assessment of permanent implants using tumour repopulation factors in the linear-quadratic model. Br J Radiol 1989;62:241–4.
66. Hendry JH, Thames HD. Fractionation sensitivity and the oxygen effect. Br J Radiol 1990;63:79–80.
67. Horsman MR. Hypoxia in tumours: Its relevance, identification and modification. In: Beck-Bornholdt HP, editor. Current topics in clinical radiobiology of tumours. Berlin: Springer-Verlag, 1993:99–112.
68. Hodgkiss RJ, Webster L, Wilson GD. Development of bioreductive markers for tumour hypoxia. Acta Oncol 1995;34:351–5.
69. Thomlinson RH, Gray LH. The histological structure of some human lung cancers and the possible implications for radiotherapy. Br J Cancer 1955;9:539–49.
70. Kolstad P. Vascularisation, oxygen tension and radiocurability in cancer of the cervix. In: Norwegian Monographs on Medical Sciences, Oslo: Scandinavian University Books, 1968.

71. Vaupel P, Schlenger K, Knoop C, Hockel M. Oxygenation of human tumours: Evaluation of tissue oxygen distribution in breast cancers by computerised O_2 tension measurements. Cancer Res 1991;51:3316–22.
72. Williams MV, Denekamp J, Fowler JF. A review of α/β values for experimental tumours: implications for clinical studies of altered fractionation. Int J Radiat Oncol Biol Phys 1985;11:87–96.
73. Revesz L, Palcic B. Radiation dose dependence of the sensitisation of oxygen and oxygen mimic sensitizers. Acta Radiol Oncol 1985;24:209–17.
74. Marples B, Joiner MC, Skov KA. The effect of oxygen on low dose hypersensitivity and radioresistance in Chinese hamster V79-379A cells. Radiat Res 1994;138:S17–S20.
75. Hall EJ. Radiation dose rate: a factor of importance in radiobiology and radiotherapy. Br J Radiol 1972;45:81–97.
76. Rojas A, Hirst VK, Calvert AS, Johns H. Carbogen and Nicotinamide as radiosensitizers in a murine mammary carcinoma using conventional and accelerated radiotherapy. Int J Radiat Oncol Biol Phys 1996;34:357–65.
77. Howes AE. An estimation of changes in the proportion and absolute numbers of hypoxic cells after irradiation of transplanted C_3H mouse mammary tumours. Br J Radiol 1969;42:441–7.
78. Dale RG, Jones B, Coles IP. The effect of tumour shrinkage on the radiobiological effectiveness of permanent brachytherapy implants. Br J Radiol 1994;67:639–45.
79. Dale RG, Jones B. The effect of tumour shrinkage on biologically effective dose, and possible implications for fractionated high dose brachytherapy. Radiother Oncol 1994;33:125–32.
80. Adams GE. Failla Memorial Lecture: Redox, radiation and reductive bioactivation. Radiat Res 1992;132:129–39.
81. Dische S. Chemical sensitisers for hypoxic cells: a decade of experience in clinical radiotherapy. Radiother Oncol 1985;3:97–115.
82. Sealy R, Korrubel J, Cridland S, Blekkenhorst G. Interstitial misonidazole: A preliminary report on a new perspective in clinical radiation sensitisation and hypoxic cell chemotherapy. Cancer 1984; 54:1535–40.
83. Balmukhanov SB, Beisebaev AA, Aitkoolova ZI, Mustaphin JS, et al. Intratumoral and parametrial infusion of metronidazole in the radiotherapy of uterine cervix cancer: preliminary report. Int J Radiat Oncol Biol Phys 1989;16:1061–3.
84. Balmukhanov SB, Beisebaev AA, Mustaphin DS, Aitkolova ZK, et al. Topical infusion of metronidazole in the radiotherapy of tumours of the uterine cervix: interim report on the 2 year survival. Br J Radiol 1990;63:499–500.
85. Hall EJ. Radiobiological measures with californium-252. Br J Radiol 1970;43:263–6.
86. Yi PN, Stanley WS, Lee W. Relationship between mitotic delay and the minimum dose rate of X-irradiation required to stop cell proliferation. Radiat Res 1993;133:163–9.
87. Zaider M, Minerbo GN. A mathematical model for cell cycle progression under continuous low dose rate irradiation. Radiat Res 1993; 133:20–6.
88. Mitchell JB, Bedford JS, Bailey SM. Dose-rate effects on the cell cycle and survival of S3 HeLa and V79 cells. Radiat Res 1979;79:520–36.
89. Morris GM. Review article: Effects of radiation on the cell proliferation kinetics of epithelial tissues—therapeutic implications. Br J Radiol 1996; 69:795–803.
90. Bissonnette RP, Echeverri F, Mahboubi A, Green DR. Apoptotic cell death induced by *c-myc* is inhibited by *bcl-2*. Nature 1992;359:552–4.
91. Milner J. DNA damage, p53 and anticancer therapies. Nature Med 1995;1:879–80.
92. Bristow RG, Benchimol S, Hill RP. The p53 gene as a modifier of intrinsic radiosensitivity: implications for radiotherapy. Radiother Oncol 1996;40:197–223.
93. Haas-Kogan DA, Yount G, Haas M, Levi D, et al. p53 dependent G1 arrest and p53 independent apoptosis influence on the radiobiological response of glioblastoma. Int J Radiat Oncol Biol Phys 1996;36:95–103.
94. Kinzler KW, Vogelstein A. Cancer-susceptibility genes: Gatekeepers and caretakers. Nature 1997;386:761–3.
95. Sharan SK, Morimatsu M, Albrecht U, et al. Embryonic lethality and radiation hypersensitivity mediated by Rad51 in mice lacking *Brca2*. Nature 1997;386:804–10.
96. Bergh J, Norberg T, Sjögren S, Lindgren A, et al. Complete sequencing of the p53 gene provides prognostic information in breast cancer patients, particularly in relation to adjuvant systemic therapy and radiotherapy. Nature Med 1995;1: 1029–34.
97. Graeber TG, Peterson JF, Tsai M, Monica K, et al. Hypoxia induces accumulation of p53 protein but activation of a G1 phase checkpoint by low oxygen conditions is independent of p53 status. Mol Cell Biol 1994;14:6264–77.
98. Ling CC, Chen CH, Fuks Z. An equation for the dose response of radiation-induced apoptosis: Possible incorporation with the LQ model. Radiother Oncol 1994;33:17–22.
99. Ling CC, Chen CH, Li WX. Apoptosis induced at different dose rates: implication for the shoulder region of cell survival curves. Radiother Oncol 1994;32:129–36.
100. Olsen DR. Calculation of the biological effect of fractionated radiotherapy: the importance of radiation induced apoptosis. Br J Radiol 1995;68:1230–6.
101. Webb A, Cunningham D, Cotter F, Clark PA, et al. BCL-2 antisense therapy in patients with non-Hodgkin's lymphoma. Lancet 1997;349:1137–41.
102. Levine EL, Davidson SE, Roberts SA, et al. Apoptosis as predictor of response to radiotherapy in cervical carcinoma. Lancet 1994;344:472.
103. Steel GG. The dose-rate effect: brachytherapy. In: Steel GG, editor. Basic clinical radiobiology (2nd edn). London: Edward Arnold, 1997:163–72.
104. Niemierko A, Goitein M. Calculation of normal tissue complication probability and dose volume histogram reduction schemes for tissues with a critical element architecture. Radiother Oncol 1991;20:166–76.
105. Niemierko A, Goitein M. Modelling of normal tissue response to radiation: the critical volume model. Int J Radiat Oncol Biol Phys 1993;25:135–45.
106. Roeske JC, Mundt AJ, Halpern H, Sweeney P, et al. Late rectal sequelae following definitive radiation therapy for carcinoma of the uterine cervix: a dosimetric analysis. Int J Radiat Oncol Biol Phys 1997;37:351–8.

107. Dale RG, Coles IP, Deehan C, O'Donoghue J. The calculation of integrated biological response in brachytherapy. Int J Radiat Oncol Biol Phys 1997;38:633–42.
108. Joslin CAF. The future of brachytherapy. In: Mould RF, Battermann JJ, Martinez AA, Speiser BL, editors. Brachytherapy from radium to optimization. Leersum, The Netherlands: Nucletron International BV, 1994:415–23.
109. Orton CG, Seyedsadr M, Somnay A. A comparison of high and low dose-rate remote afterloading for cervix cancer and the importance of fractionation. Int J Radiat Oncol Biol Phys 1991;21:1425–34.
110. Scalliet P, Vanneste F, Octave-Prignot M. Do steeping sources differ from linear sources regarding their biological effectiveness? In: Proceedings of GEC/ESTRO Meeting, Stockholm, 1997:S7.
111. Jones B, Tan LT, Blake PR, Dale RG. Results of a questionnaire regarding the practice of radiotherapy for carcinoma of the cervix in the UK. Br J Radiol 1994;67:1226–30.
112. Newman G. Increased morbidity following the introduction of remote afterloading, with increased dose rate, for cancer of the cervix. Radiother Oncol 1996;39:97–103.
113. Stitt JA, Fowler JF, Thomadsen BR, Buchler DA, et al. High dose rate intracavitary brachytherapy for carcinoma of the cervix: The Madison System. 1. Clinical and radiobiological considerations. Int J Radiat Oncol Biol Phys 1992;24:335–48.
114. Dale RG. The use of small fraction numbers in high dose-rate gynaecological afterloading: some radiobiological considerations. Br J Radiol 1990;63:290–4.
115. Ling CC, Sahoo N, Liebel S, Anderson LL. High dose-rate gynecological applications—radiobiological considerations based on the α–β model. Radiother Oncol 1992;25:103–10.
116. Roy JN, Anderson LL, Wallner KE, Fuks Z, et al. Tumor control probability for permanent implants in prostate. Radiother Oncol 1993;28:72–5.
117. Jacobs H. Breast conserving therapy: experience with HDR afterloading iridium implants. In: Martinez AA, Orton CG, Mould RF, editors. Brachytherapy HDR and LDR. Leersum, The Netherlands: Nucletron BV, 1990:251–6.
118. Brenner DJ, Hall EJ. Fractionated high dose-rate *versus* low dose-rate regimens for intracavitary brachytherapy of the cervix. Br J Radiol 1991;64:133–41.
119. Orton CG, Brenner DJ, Dale RG, Fowler JF. Radiobiology. In: Nag S, editor. High dose-rate brachytherapy—A Textbook, Amonk, NY: Futura Publishing Company, 1994:11–26.
120. Hall EJ. Dose rate considerations. In: Mould RF, Battermann JJ, Martinez AA, Speiser BL, editors. Brachytherapy from radium to optimization. Leersum, The Netherlands: Nucletron International BV, 1994:9–18.
121. Deehan C, O'Donoghue JA. Biological equivalence of LDR and HDR brachytherapy. In: Mould RF, Battermann JJ, Martinez AA, Speiser BL, editors. Brachytherapy from radium to optimization. Leersum, The Netherlands: Nucletron International BV, 1994:19–33.
122. Jones B, Tan LT, Dale RG. Derivation of the optimum dose per fraction from the linear quadratic model. Br J Radiol 1995;68:894–902.
123. Fowler JF, Van Limbergen EFM. Biological effect of pulsed dose rate brachytherapy with stepping sources if short half-times of repair are present in tissues. Int J Radiat Oncol Biol Phys 1997;37:877–83.
124. Fowler JF, Mount M. Pulsed brachytherapy: The conditions for no significant loss of therapeutic ratio compared with traditional low dose-rate brachytherapy. Int J Radiat Oncol Biol Phys 1992;23:661–9.
125. Brenner DJ, Hall EJ. Conditions for the equivalence of continuous to pulsed low dose rate brachytherapy. Int J Radiat Oncol Biol Phys 1991;20:181–90.
126. Galelli M, Feroldi P. The time variable dose-rate in HDR stepping source brachytherapy. Radiother Oncol 1993;27:173–4.
127. Chen C-Z, Huang Y, Hall EJ, Brenner EJ. Pulsed brachytherapy as a substitute for continuous low dose-rate: An *in vitro* study with human carcinoma cells. Int J Radiat Oncol Biol Phys 1997;37:137–43.
128. Visser AG, Van Den Aardweg GJMJ, Levendag PC. Pulsed dose rate and fractionated high dose rate brachytherapy: Choice of brachytherapy schedules to replace low dose rate treatments. Int J Radiat Oncol 1996;34:497–505.
129. Fowler JF. Why shorter half-times of repair lead to greater damage in pulsed brachytherapy. Int J Radiat Oncol Biol Phys 1993;26:353–6.
130. Fowler JF. Are half-times of repair reliably shorter for tumors than for late normal tissue effects? Int J Radiat Oncol Biol Phys 1995;31:189–90.
131. Haustermans K, Fowler J, Landuyt W, Lambin P, et al. Is pulsed dose rate more damaging to spinal cord of rats than continuous low dose rate? Radiother Oncol 1997;45:39–47.
132. Hall EJ, Brenner DJ. Pulsed dose-rate brachytherapy (editorial). Radiother Oncol 1997;45:1–2.
133. Dale RG, Huczkowski J, Trott KR. Possible dose rate dependence of recovery kinetics as deduced from a preliminary analysis of the effects of fractionated irradiations at varying dose rates. Br J Radiol 1988;61:153–7.
134. Brenner DJ, Hall EJ, Huang Y-P, Sachs RK. Potential reduced late effects for pulsed brachytherapy compared with conventional LDR. Int J Radiat Oncol Biol Phys 1995;31:201–2.
135. Brenner DJ, Hall EJ, Randers-Pehrson G, Huang Y-P, et al. Quantitative comparisons of continuous and pulsed dose-rate regimens in a model late-effect system. Int J Radiat Oncol Biol Phys 1996;34:905–10.
136. Pop LAM, Van Den Broek JFCM, Visser AF, Van Der Kogel AJ, et al. Constraints in the use of repair half-times and mathematical modelling for the clinical application of HDR and PDR treatment schedules as an alternative for LDR brachytherapy. Radiother Oncol 1996;38:153–62.
137. Dale RG, Loft SM, Coles IP. The potential of ytterbium-169 in brachytherapy, a brief physical and radiobiological assessment. Br J Radiol 1992;65:252–7.
138. Mason DL, Battista JJ, Barnett RB, Porter AT. Ytterbium-169: Calculated physical properties of a new radiation source for brachytherapy. Med Phys 1992;19:695–703.
139. Dale RG. Time-dependent tumour repopulation factors in the linear quadratic equations—implications for treatment strategies. Radiother Oncol 1989;15:371–81.
140. Ling CC. Permanent implants using Au-198, Pd-103 and I-125: radiobiological considerations based on the linear-quadratic model. Int J Radiat Oncol Biol Phys 1992;23:81–7.

141. Kreth FW, Faist M, Rossner R, Birg W, et al. The risk of interstitial radiotherapy of low-grade gliomas. Radiother Oncol 1997;43:253–60.
142. Jones B, Bleasdale CM. Effect of overall time when radiotherapy includes teletherapy and brachytherapy: a mathematical model. Br J Radiol 1994;67:63–70.
143. Tan LT, Jones B, Green JA, Kingston RE, Clark PI. Treatment of carcinomas of the uterine cervix which remain bulky after initial external beam radiotherapy: a pilot study using integrated cytotoxic chemotherapy prior to brachytherapy. Br J Radiol 1996;69:165–71.
144. Deehan C, O'Donoghue JA. Biological equivalence between fractionated radiotherapy treatments using the linear-quadratic model. Br J Radiol 1988;61:1187–8.
145. Tan LT, Jones B, Freestone G, Dale RG. Case report: Low dose rate and high dose rate intracavitary brachytherapy in a patient with carcinoma of the cervix. Br J Radiol 1996;69:84–6.
146. Jones B, Dale RG. Cell loss factors and the linear-quadratic model. Radiother Oncol 1995;37:136–9.
147. Sahoo N, Ling CC, Anderson LL. Analysis of factors affecting the therapeutic gain in high dose-rate gynecological implants relative to low dose-rate implants. Med Phys 1996;23:419–25.
148. Rodrigus P, De Winter K, Venselaar JLM, Leers WH. Evaluation of late morbidity in patients with carcinoma of the uterine cervix following a dose rate change. Radiother Oncol 1997;42:137–41.
149. Velculescu VE, Zhang L, Vogelstein B, Kinzler KW. Serial analysis of gene expression. Science 1995;270:484–7.
150. Yarnold J. Molecular aspects of cellular responses to radiotherapy. Radiother Oncol 1997;44:1–7.

Appendices: Radiobiological equations for application in brachytherapy

Appendix A: HDR brachytherapy

For an HDR fractionated treatment consisting of N fractions of magnitude d, BED is defined as BED = Total Dose × Relative Effectiveness, *i.e.*

$$\mathrm{BED} = Nd\left[1 + \frac{d}{(\alpha/\beta)}\right] \tag{A1}$$

If the overall treatment time is T days, then the tumour BED may be corrected for concurrent tumour repopulation via:

$$\mathrm{BED} = Nd\left[1 + \frac{d}{(\alpha/\beta)}\right] - KT \tag{A2}$$

where K is the dose equivalent of daily repopulation, defined in terms of intrinsic radiosensitivity (α) and potential doubling time (T_{pot}) as:

$$K = \frac{0.693}{\alpha T_{\mathrm{pot}}} \tag{A3}$$

Appendix B: CLDR brachytherapy

For a CLDR regime delivered at dose-rate R over time T, the formula for finding BED is:

$$\mathrm{BED} = RT\left[1 + \frac{2R}{\mu(\alpha/\beta)}\left(1 - \frac{1}{\mu T}(1 - \mathrm{e}^{-\mu T})\right)\right] \tag{B1}$$

where μ is the recovery constant (assumed to be mono-exponential) of sub-lethal damage.

When T is very short, Equation (B1) is equivalent to Equation (A1). For increasingly longer values of T Equation (B1) successively simplifies to:

$$\mathrm{BED} = RT\left[1 + \frac{2R}{\mu(\alpha/\beta)}\left(1 - \frac{1}{\mu T}\right)\right] \tag{B2}$$

and then to:

$$\mathrm{BED} = RT\left[1 + \frac{2R}{\mu(\alpha/\beta)}\right] \tag{B3}$$

In cases where there is a multiphasic repair process consisting of m exponentially repairing components with respective proportions a_i, such that:

$$\sum_{i=1}^{m} a_i = 1$$

then the fraction of sub-lethally damaged lesions at time t is

$$\sum_{i=1}^{m} a_i \mathrm{e}^{-\mu t_i} \tag{B4}$$

and Equation (B1) becomes:

$$\mathrm{BED} = RT\left[1 + \frac{2R}{(\alpha/\beta)}\sum_{i=1}^{m}\left(\frac{a_i}{\mu_i}\right)\left(1 - \frac{1 - \mathrm{e}^{-\mu_i T}}{\mu_i T}\right)\right] \tag{B5}$$

Equation (B5) may be derived by following the method of Dale [32].

For increasingly longer values of T, Equation (B4) successively simplifies to:

$$\mathrm{BED} = RT\left[1 + \frac{2R}{(\alpha/\beta)}\sum_{i=1}^{m}\left(\frac{a_i}{\mu_i}\right)\left(1 - \frac{1}{\mu_i T}\right)\right] \tag{B6}$$

and then to:

$$\mathrm{BED} = RT\left[1 + \frac{2R}{(\alpha/\beta)}\sum_{i=1}^{m}\left(\frac{a_i}{\mu_i}\right)\right] \tag{B7}$$

Appendix C: Pulsed brachytherapy

For N closely-spaced pulses, each of dose rate R and duration T, the BED is calculated from:

$$\mathrm{BED} = NRT\left[1+\frac{2R}{\mu(\alpha/\beta)}\left(1-\frac{NY-SY^2}{N\mu T}\right)\right] \tag{C1}$$

where:

$$S=\frac{NK-K-NK^2Z+K^{N+1}Z^N}{(1-KZ)^2}$$

$$Z=\mathrm{e}^{-\mu T};\quad Y=1-Z;\quad K=\mathrm{e}^{-\mu X}$$

and X is the radiation-free interval between pulses.

Equation (C1) assumes mono-exponential recovery kinetics. Where there is multiphasic recovery the method of Haustermans et al may be used to find the "effective" RE, the square bracketed term in Equation (C1) being summed over all contributing half-lives, each weighted according to the fractional preponderance of the particular half-lives. If the recovery is bi-phasic and if the individual pulses are not each of the same magnitude, the more complex equations of Millar et al [54] should be used. When re-written in the above form these become:

$$\mathrm{BED} = D_T+\frac{1}{\alpha/\beta}\left[a_1\phi(\Xi,\mu_1)+a_2\phi(\Xi,\mu_2)\right]\sum_{k=1}^{N} {d_k}^2 \tag{C2}$$

where:

$$\phi(\Xi,\mu)=\frac{2}{\mu}\frac{\sum_{j=1}^{N}\{V-W\}}{\sum_{k=1}^{N} {d_k}^2}$$

$$V={d_j}^2\frac{\left\{\delta t_j-\frac{1}{\mu}\left[1-\exp(-\mu\delta t_j)\right]\right\}}{\delta t_j^2}$$

$$W=\frac{1}{\mu}\sum_{i=1}^{j-1} d_i d_j\left(\frac{1}{\delta t_i\delta t_j}\right)\exp\left[-\mu(t_j-t_i)\right]\times\left[\exp(\mu dt_i)-1\right]\times\left[\exp(-\mu\delta t_j)-1\right]$$

t_i is the time at which the ith fraction begins, δt_i is irradiation duration of the ith fraction, and d_k is the dose delivered in the kth fraction.

Appendix D: Brachytherapy involving decaying sources

For a permanent implant delivering an initial dose rate of R_0, and involving a nuclide with decay constant λ, BED is given as:

$$\mathrm{BED}=\frac{R_0}{\lambda}\left(1+\frac{R_0}{(\mu+\lambda)(\alpha/\beta)}\right) \tag{D1}$$

For a non-permanent implant with a decaying source, removed after time T:

$$\mathrm{BED}=\frac{R_0}{\lambda}\left(1-\mathrm{e}^{-\lambda T}\right)\left[1+\frac{2R_0\lambda}{(\mu-\lambda)(\alpha/\beta)}\right]\left(\frac{A-B}{C}\right) \tag{D2}$$

where:

$$A=\frac{1}{2\lambda}\left[1-\mathrm{e}^{-2\lambda T}\right]$$

$$B=\frac{1}{(\mu+\lambda)}\left[1-\mathrm{e}^{-(\mu+\lambda)T}\right]$$

$$C=1-\mathrm{e}^{-\lambda T}$$

Appendix E: The incorporation of tumour shrinkage effects

If the tumour shrinks exponentially with rate constant z during the period of treatment then, for HDR:

$$\mathrm{BED}=NdX\left[1+X\frac{d}{(\alpha/\beta)}\right] \tag{E1}$$

where:

$$X=1+(N-1)zt$$

and t is the average elapsed time between each fraction.

For CLDR delivered over many hours:

$$\mathrm{BED}=RTY\left[1+\frac{2RY}{\mu(\alpha/\beta)}\right] \tag{E2}$$

where $Y=1+zT$.

(Note the respective correspondence between Equations (E1) and (A1), and Equations (E2) and (B3)).

For a permanent implant within a shrinkage tumour:

$$\mathrm{BED}=\frac{R_0}{\lambda}\left(1-\mathrm{e}^{-\lambda T_{\mathrm{eff}}}\right)\left[1+\frac{2R_0(\lambda-2z)}{(\mu-\lambda+2z)(\alpha/\beta)}\right]\times\left[A(B-C)\right] \tag{E3}$$

where in this case:

$$A=\frac{1}{\left(1-\mathrm{e}^{(2z-\lambda)T_{\mathrm{eff}}}\right)}$$

$$B=\frac{1}{2(\lambda-2z)}\left[1-\mathrm{e}^{-2(2z-\lambda)T_{\mathrm{eff}}}\right]$$

$$C=\frac{1}{(\mu+\lambda-2z)}\left[1-\mathrm{e}^{-(\mu+\lambda-2z)T_{\mathrm{eff}}}\right]$$

and:

$$T_{\mathrm{eff}}=-\frac{\left[\ln\left(\frac{K}{R_0}\right)\right]}{(\lambda-2z)}$$

For longer-lived radionuclides, R_0 is generally small, and Equation (E3) simplifies to:

$$\mathrm{BED} \cong \frac{\left[R_0 - K + K \ln\left(\frac{K}{R_0}\right)\right]}{(\lambda - 2z)} \qquad \text{(E4)}$$

Appendix F: The determination of optimum dose per fraction

When the tumour and critical normal tissue each receive the same total dose and dose/fraction, the optimum dose/fraction (d) may be determined as the solution of:

$$(\beta k T_{\mathrm{pot}} - \alpha T_{\mathrm{pot}})d^2 + 1.386fd + 0.693fk = 0 \qquad \text{(F1)}$$

where α and β are the respective linear and quadratic radiosensitivity coefficients for the tumour, T_{pot} is the tumour potential doubling time, k is the α/β ratio for the critical normal tissue. Factor f is the average time interval between each fraction, obtained by dividing the number of fractions delivered each week into 7.

Where normal tissue sparing occurs, with the normal tissue receiving fraction g of the dose to the tumour ($g<1$), the optimum tumour dose/fraction (z) is the solution of:

$$(Bk T_{\mathrm{pot}} - \alpha g T_{\mathrm{pot}})z^2 + 1.386fgz + 0.693fk = 0 \qquad \text{(F2)}$$

Since the daily dose equivalent of repopulation for the tumour is given by Equation (A3), Equations (F1) and (F2) may be simplified by dividing throughout by αT_{pot}, and substituting K (the dose-equivalent of the repopulation rate in Gy day^{-1}) where appropriate, *i.e.* Equation (F1) becomes:

$$\left(1 - \frac{(\alpha/\beta)_{\mathrm{late}}}{(\alpha/\beta)_{\mathrm{tum}}}\right)d^2 - 2fKd - (\alpha/\beta)_{\mathrm{late}} fK = 0 \qquad \text{(F3)}$$

and Equation (E2) becomes:

$$\left(g - \frac{(\alpha/\beta)_{\mathrm{late}}}{(\alpha/\beta)_{\mathrm{tum}}}\right)z^2 - 2fgKz - (\alpha/\beta)_{\mathrm{late}} fK = 0 \qquad \text{(F4)}$$

Although respectively identical to Equations (F1) and (F2), the last two equations are easier to use because they do not require individual values of α, β and T_{pot} to be known.